Available online at www.sciencedirect.com
SCIENCE DIRECT®
PERGAMON
Polyhedron 22 (2003) 1535–1545
POLYHEDRON
www.elsevier.com/locate/poly

Synthesis and characterization of axial coordination cobalt(III) complexes containing chiral Salen ligands

Yu-Ling Zhang, Wen-Juan Ruan *, Xiao-Jing Zhao, Hong-Gen Wang, Zhi-Ang Zhu

Department of Chemistry, Nankai University, Tianjin 300071, China

Received 3 December 2002; accepted 14 March 2003

Abstract

Cobalt(III) complexes containing both optically active tetradentate Schiff base ligands, (SB = Salen, MeOSalen, *t*-Bu-Salen) with axial ligands (L) $[Co(SB)L_2]ClO_4$ (L = imidazole (Im), 2-methylimidazole (2-MeIm), 1-methylimidazole (MeIm)) have been prepared and characterized. In addition, the crystal structures of $[Co(Salen)(MeIm)_2]ClO_4$ (**1c**), $[Co(MeOSalen)(MeIm)_2]ClO_4$ (**2c**), and $[Co(t\text{-Bu-Salen})(MeIm)_2]ClO_4$ (**3c**) have been determined by X-ray structure analysis. The properties of these hexacoordinate complexes, such as electronic absorption, circular dichroism spectra, and ^1H NMR spectra, have been studied.

Keywords: Salen ligands; Axial coordination cobalt(III) complexes; Circular dichroism spectra (CD); X-ray structures

1. Introduction

Cobalt Schiff base complexes have been used as catalysts for the oxygenation reactions of organic molecules [1], the reversibility of which is closely related to the redox potential of the Co(III)/Co(II) couple [2]. On the other hand, the cobalt complexes with tetradentate Schiff base ligands have been extensively used to mimic cobalamin (B_{12}) coenzymes [3–6], dioxygen carriers and oxygen activators [7–9]. In addition, the discovery that cobalt(III) Schiff base complexes are potent antiviral agents prompted us to initiate an investigation of Co(III) interactions with proteins and nucleic acids. Co(III) Schiff base complexes with two amines in axial positions have been used as antimicrobial agents as well [10].

Salen complexes as a chiral Schiff base have been used in asymmetric catalytic and electrochemical catalytic reactions in recent years. In asymmetric catalytic reactions, both the geometry and the redox potential of chiral Salen cobalt complexes affect the enantioselectivity [11]. The reversible oxygen transport by cobalt Schiff base complexes is widely studied [12]. Generally, Schiff base complexes of cobalt are used in oxidative coupling catalytic reactions of phenols and oxidation of olefins. The influence of stereo isomerism or optical isomerism in Schiff base cobalt complexes on the catalysis of the oxidation of some organic compounds, organic synthesis and the asymmetric hetero-Diels–Alder reaction [13,14] stimulated us to study their chemical, thermal and electrochemical behavior. In this paper, we report the synthesis and spectroscopic characterization of several cobalt(III) complexes with a chiral Schiff base (Salen) and axial ligands (Fig. 1). In addition, the crystal structures of cobalt complexes $[Co(Salen)(MeIm)_2]ClO_4$ (**1c**), $[Co(MeOSalen)(MeIm)_2]ClO_4$ (**2c**) and $[Co(t\text{-Bu-Salen})(MeIm)_2]ClO_4$ (**3c**) (Fig. 1) are studied and the cobalt(III) complexes are discussed based on the UV–Vis, CD and ^1H NMR spectra.

2. Experimental

2.1. Physical measurements

The ^1H NMR spectra were recorded on a Mercury Vx300 spectrometer (300 MHz) at room temperature

* Corresponding author. Fax: +86-22-235-02458.
E-mail address: wjruan@nankai.edu.cn (W.-J. Ruan).

0277-5387/03/$ - see front matter © 2003 Elsevier Science Ltd. All rights reserved.
doi:10.1016/S0277-5387(03)00261-4

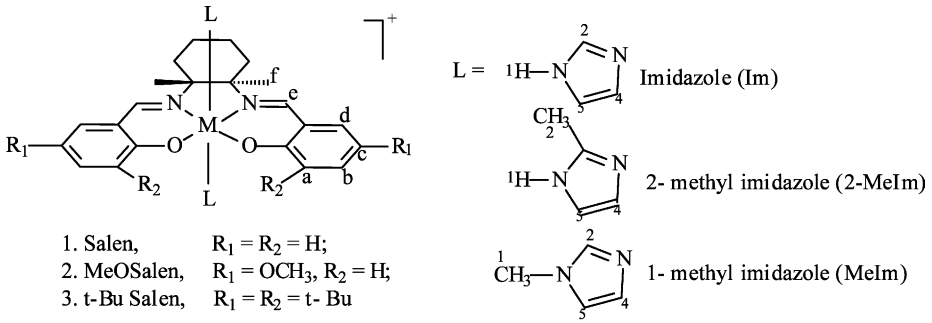

Fig. 1. The structure of complexes **1**, **2** and **3**.

using methanol as solvent and tetramethylsilane as internal standard. Elemental analyses (C, H, N) were made on a Perkin-Elemer 240 spectrometer automatic analyzer. The IR spectra of solid samples were recorded in the range of 4000–400 cm^{-1} on a Bio-Rad 135 FT-IR spectrophotometer as KBr pellets. CD spectra were recorded with a JASCO-715 spectrometer and the UV–Vis spectrum was measured on a U-3010 spectrophotometer, in the range of 200–600 nm. All spectra were recorded in CH_2Cl_2 solution at room temperature. Crystal structure analysis was carried out on a Bruker Smart 1000 CCD diffractometer.

2.2. Synthesis

2.2.1. Synthesis of ligands

(*R*, *R*)-1,2-Diaminocyclohexane was prepared by modification of the reported method [15,16]. *Cis*/*trans*-1,2-diaminocyclohexane were resolved by L-(+)tartaric acid and its tartrate was obtained. Salen (**1**) (*N*,*N*′-disalicylidene-1,2-diminocyclohexane), MeOSalen (**2**) (di-5-methoxy-salicylidene-1,2-diminocyclohexane), *t*-Bu-Salen (**3**) (di-3,5-*tert*-butyl-salicylidene-1,2-diminocyclohexane) ligands were prepared by the literature method [15].

*2.2.1.1. Salen (**1**). Anal*. Found: C, 74.53; H, 6.83; N, 8.70. Calc. for $C_{20}H_{22}O_2N_2$, C, 74.20; H, 6.65; N, 8.60%. ^1H NMR ($CHCl_3$, 300 MHz) (ppm) $\delta = 13.1$(b, O–H); 8.21(d, 2H, CH=N); 7.21 (d, 2H, Ar–H); 7.14 (d, 2H, Ar–H); 6.87(d, 2H, Ar–H); 6.75 (d, 2H, Ar–H); 3.34 (s, chiral H); 1.91–1.41(m, 8H, CH_2). UV–Vis λ_{max} (nm) (log(ε, M^{-1} cm^{-1})) (CH_2Cl_2): 318 (3.42); 256 (3.82). CD λ_{max} (nm), ($\Delta\varepsilon$, M^{-1} cm^{-1}) (CH_2Cl_2): 353 (−126.9).

*2.2.1.2. MeOSalen (**2**). Anal*. Found: C, 69.11; H, 6.81; N, 7.33. Calc. for $C_{22}H_{26}O_4N_2$, C, 68.86; H, 6.92; N, 7.25%. ^1H NMR ($CHCl_3$, 300 MHz) (ppm) $\delta = 13.01$(b, OH); 8.32 (s, 2H, CH=N); 6.92–6.88 (m, 2H, Ar–H); 6.80–6.76 (t, 4H, Ar–H); 3.72 (s, 6H, OCH_3); 3.42–3.38 (m, 2H, chiral H); 2.01–1.59 (m, 8H, $(CH_2)_4$). UV–Vis λ_{max} (nm), (log(ε, M^{-1} cm^{-1})) (CH_2Cl_2): 345.6 (3.75); 258.8 (4.47); 231.0 (4.34). CD λ_{max} (nm), ($\Delta\varepsilon$, M^{-1} cm^{-1}), (CH_2Cl_2): 383 (−93.81); 300(−22.35); 283 (+53.81).

*2.2.1.3. t-Bu-Salen (**3**). Anal*. Found: C, 79.10; H, 9.80; N, 5.34. Calc. for $C_{36}H_{54}N_2O_2$, C, 79.12; H, 9.89; N, 5.13%. ^1H NMR ($CHCl_3$, 300 MHz) (ppm) $\delta = 8.31$ (s, 2H, CH=N); 7.31 (s, 2H, Ar–H); 7.99 (s, 2H, Ar–H); 3.34 (s, 2H, chiral H); 2.97–1.47 (m, 8H, CH_2); 1.41 (s, 9H, *t*-Bu); 1.24 (s, 9H, *t*-Bu). UV–Vis λ_{max} (nm) (log(ε, M^{-1} cm^{-1})) (CH_2Cl_2): 330 (3.92); 260 (4.33); 239 (4.28). CD λ_{max} (nm) ($\Delta\varepsilon$, M^{-1} cm^{-1}), (CH_2Cl_2): 382 (−33.67).

2.2.2. Synthesis of cobalt complexes

*2.2.2.1. [Co(Salen)(Im)$_2$]ClO$_4$ complex (**1a**).* To an ethanol solution (6 ml) of the ligand Salen (0.173 g, 0.5 mmol) and imidazole (0.115 g, 1.6 mmol) was added an ethanol solution (1.5 ml) of NaOH (30 mg, 0.75 mmol) and $Co(CH_3COO)_2 \cdot 4H_2O$ (0.136 g, 0.6 mmol). The reaction mixture was stirred for 8 h at room temperature to give a red solution. An ethanol solution (7 ml) of $NaClO_4 \cdot H_2O$ (0.42 g, 3 mmol) was then added and the mixture was stirred for 2 h. The resulting red precipitate was collected by filtration and recrystallized by dichloromethane–methanol. The product was dried under vacuum. Yield: 75.5%. *Anal*. Found: C, 49.86; H, 5.32; N, 12.65. Calc. for $C_{26}H_{28}O_2N_6Co_1 \cdot ClO_4 \cdot CH_3OH$: C, 50.12; H, 4.95; N, 12.99%. FT-IR, (KBr, cm^{-1}): 3142 (w, Im ring), 3050 (w, Ar–H), 2938 (m), 2860 (w, H–C–H), 1633 (vs, C=N), 1602 (s), 1537 (m, Ar, C=C), 1453 (vs, Ar–H); 1320 (s, C–N), 1246 (s, Ar C–C), 1089 (vs), 624 (s, ClO_4^-), 567 (m, M–N), 498 (m), 470 (w, M–O). UV–Vis: λ_{max} (nm) (log(ε, M^{-1} cm^{-1})) (CH_2Cl_2): 394 (3.84), 259 (4.81), 230 (4.72). CD:λ_{max} (nm) ($\Delta\varepsilon$, M^{-1} cm^{-1}), (CH_2Cl_2): 527 (+59.8), 405 (−95.7), 353 (−16.9), 323 (−37.6), 299 (−26.6), 284 (−31.9).

*2.2.2.2. [Co(Salen)(2-MeIm)$_2$]ClO$_4$ complex (**1b**).* This red brown complex was prepared by the same method as for **1a** except that 2-methylimidazole was

used instead of imidazole. Recrystallization was carried out from chloroform–methanol. Yield: 62.1%. *Anal.* Found: C, 45.66; H, 4.30; N, 10.57. Calc. for $C_{28}H_{32}O_2N_6Co_1\cdot ClO_4\cdot CHCl_3$: C, 45.67; H, 4.33; N, 11.02%. FT-IR (KBr, cm^{-1}): 3130 (w, Im ring), 3047 (w, Ar–H), 2927 (m), 2865 (w, H–C–H), 1625 (vs, C=N), 1601 (s), 1568, 1534 (m, Ar C=C), 1451 (vs, Ar–H), 1350 (m), 1318 (s, C–N), 1247 (s, Ar C–C), 1108 (vs), 623 (s, ClO_4^-), 567 (m, M–N), 470 (m), 425 (w, M–O). UV–Vis λ_{max} (nm) ($\log(\varepsilon, M^{-1} cm^{-1})$) ($CH_2Cl_2$): 388 (4.00), 260.5 (4.97), 237 (4.88). CD λ_{max} (nm) ($\Delta\varepsilon$, $M^{-1} cm^{-1}$) (CH_2Cl_2): 542 (+104), 425 (−156.7), 374 (6.95), 320 (−82.6). ^1H NMR (300 MHz, CD_3OD): $\delta = 8.04$ (s, $2H_e$, CH=N), 7.27–7.24 (t, $4H_{b,c}$, Ar–H), 7.13–7.11 (d, $2H_a$, Im ring), 6.89–6.69 (s, $2H_d$, Ar–H), 6.58–6.53 (m, $2H_5$, 2-MeIm), 6.40 (s, $2H_4$, 2-MeIm), 3.57 (s, 2H, chiral H), 2.91–2.87 (d, $2H_g$, CH_2), 2.36 (s, 6H, CH_3), 2.30 (s, 2H, N–H), 1.99–1.55 (m, 6H, CH_2).

*2.2.2.3. [Co(Salen)(MeIm)$_2$]ClO$_4$ complex (**1c**).* The complex was prepared by the same method as for **1a**. Recrystallization from dichloromethane–methanol gave a dark red crystal. Yield: 55%. *Anal*. Found: C, 47.93; H, 4.40; N, 11.55. Calc. for $C_{28}H_{32}O_2N_6Co_1\cdot ClO_4\cdot CH_2Cl_2$: C, 7.90; H, 4.32; N, 11.56%. FT-IR (KBr, cm^{-1}): 3145, 3132 (m, Im ring), 3056 (w, Ar–H), 2936, 2861 (w, H–C–H), 1632 (vs, C=N), 1601, 1540 (s, Ar C=C), 1452 (vs, Ar–H), 1348 (m, C–N), 1318 (s, Ar C–C), 1244 (m, C–O), 1098 (vs, ClO_4^-), 622 (s), 567 (m, M–N), 470 (m), 458 (w, M–O). UV–Vis λ_{max} (nm) ($\log(\varepsilon, M^{-1} cm^{-1})$) ($CH_2Cl_2$): 395 (3.77), 260.7 (4.55), 232 (4.39). CD λ_{max} (nm) ($\Delta\varepsilon$, $M^{-1} cm^{-1}$) (CH_2Cl_2): 534 (+59.28), 413 (−108.3), 363 (−1.78), 330 (−57.35), 298 (−35.18). ^1H NMR (CD_3OD, 300 MHz) (ppm): $\delta = 8.16$ (s, $2H_e$, CH=N), 7.46–7.45 (d, $2H_2$, Im ring), 7.43 (s, $2H_a$, Ar–H), 7.35–7.29 (m, $2H_d$, Ar–H), 7.21–7.18 (m, $2H_c$, Ar–H), 6.97–6.95 (s, $2H_5$, MeIm), 6.68–6.56 (d, $2H_d$, Ar–H), 6.65–6.63 (m, $2H_4$, MeIm), 3.63 (s, 6H, CH_3), 3.42–3.41 (d, 2H, chiral H), 3.01–2.97 (d, 2H, CH_2), 2.07–1.57 (m, 6H, CH_2).

*2.2.2.4. [Co(MeOSalen)(Im)$_2$]ClO$_4$ complex (**2a**).* To a methanol solution of MeOSalen (0.19 g, 0.5 mmol) and imidazole (0.11 g, 1.5 mmol) was added a 0.27 mol dm^{-3} solution of NaOH (27 mg, 0.68 mmol) in methanol (2.5 ml). The yellow mixture was stirred for 1 h and $Co(CH_3COO)_2\cdot 4H_2O$ (0.133 g, 0.6 mmol) was added. The reaction mixture was stirred for 18 h at room temperature to give a red solution. A methanol solution (5 ml) of $NaClO_4\cdot H_2O$ (0.15 g) was then added and the mixture was stirred for a further 3 h. A dark red precipitate was collected by filtration and was then recrystallized from dichloromethane–methanol. Yield: 56.3%. *Anal*. Found: C, 45.93; H, 4.30; N, 11.44. Calc. for $C_{28}H_{32}O_4N_6Co_1\cdot ClO_4\cdot CH_2Cl_2$: C, 45.81; H, 4.48; N, 11.06%. FT-IR (KBr, cm^{-1}): 3242 (w), 3146 (m, Im ring), 3056 (w, Ar–H), 2939 (m), 2861, 2836 (w, H–C–H), 1632 (vs, C=N), 1537 (s, Ar C=C), 1471 (vs), 1427 (m, Ar–H), 1339 (w), 1313 (s, C–N), 1293 (m), 1260 (s, Ar C–C), 1220 (s, C–O), 1089 (vs), 623 (s, ClO_4^-), 551 (m, M–N), 499 (m), 469 (w, M–O). UV–Vis λ_{max} (nm) ($\log(\varepsilon, M^{-1} cm^{-1})$) ($CH_2Cl_2$): 429 (3.32), 260 (4.21), 237 (4.16). CD λ_{max} (nm) ($\Delta\varepsilon$, $M^{-1} cm^{-1}$) (CH_2Cl_2): 544 (+19.31), 437 (−37.77), 377 (−5.35), 339 (−11.25), 304 (−3.19), 270 (−24.81).

*2.2.2.5. [Co(MeOSalen)(2-MeIm)$_2$]ClO$_4$ complex (**2b**).* This complex was prepared by the same method as for **2a** except that ethanol was used as the solvent and 2-methylimidazole was used instead of imidazole. Recrystallization from dichloromethane–ethanol gave a dark red solid. Yield: 58%. *Anal*. Found: C, 47.33; H, 5.10; N, 10.89. Cacl. for $C_{30}H_{36}O_4N_6Co_1\cdot ClO_4\cdot CH_2Cl_2$: C, 47.24; H, 4.83; N, 10.67%. FT-IR (KBr, cm^{-1}): 3119 (m, Im ring), 3052 (w, Ar–H), 2938, 2862 (w, H–C–H), 1630 (vs, C=N), 1571, 1540 (s, Ar, C=C), 1468 (vs, Ar–H), 1358 (m, C–N), 1294 (s, Ar C–C), 1223 (m, C–O), 1108 (s), 623 (s, ClO_4^-), 553 (m, M–N), 471 (m), 421(w, M–O). UV–Vis λ_{max} (nm), ($\log(\varepsilon, M^{-1} cm^{-1})$) ($CH_2Cl_2$): 418 (3.89), 263.3 (3.61), 236 (3.58). CD λ_{max} (nm), ($\Delta\varepsilon$, $M^{-1} cm^{-1}$) (CH_2Cl_2): 578 (+8.72), 457 (−16.92), 389 (−2.17), 347 (−8.47), 323 (−6.89), 276 (−15.49). ^1H NMR (CD_3OD, 300 MHz) (ppm):$\delta = 8.05$ (s, 2H, CH=N), 7.02–7.07 (d, $2H_b$, Ar–H), 7.01 (t, $2H_d$, Ar–H), 6.86 (s, $2H_a$, Ar–H), 6.85 (s, $2H_5$, 2-MeIm), 6.454 (s, $2H_4$, Im ring), 3.80 (s, 6H, OCH_3), 3.60 (d, 2H, chiral 2H), 2.95–2.91 (d, 2H, CH_2), 2.42 (s, 6H, CH_3), 2.07–1.59 (m, 6H, CH_2).

*2.2.2.6. [Co(MeOSalen)(MeIm)$_2$]ClO$_4$ complex (**2c**).* This dark red complex was prepared by the same method as for **2a** except that 1-methylimidazole was used instead of imidazole. The product was recrystallized from dichloromethane–methanol. Yield: 60.5%. *Anal*. Found: C, 47.32; H, 4.91; N, 10.57. Cacl. for $C_{30}H_{36}O_4N_6Co_1\cdot ClO_4\cdot CH_2Cl_2$: C, 47.24; H, 4.83; N, 11.67%. FT-IR (KBr, cm^{-1}): 3137 (m, Im ring), 3055 (w, Ar–H), 2938 (m), 2862 (w), 2835 (w, H–C–H), 1630 (vs, C=N), 1537 (s, Ar C=C), 1470 (vs), 1462 (m, Ar–H), 1348 (w, C–N), 1314, 1296 (s, Ar C–C), 1219 (s, C–O), 1097 (vs), 622 (s, ClO_4^-), 551 (w, M–N), 496 (w), 470 (w, M–O). UV–Vis λ_{max} (nm) ($\log(\varepsilon, M^{-1} cm^{-1})$) ($CH_2Cl_2$): 430 (3.87), 263 (4.15), 236 (4.00). CD λ_{max} (nm), ($\Delta\varepsilon$, $M^{-1} cm^{-1}$) (CH_2Cl_2): 567 (+13.28), 444 (−32.48), 381 (−2.32), 339 (−10.78), 314 (−6.57), 254 (−4.16), 240 (−6.18). ^1H NMR (CD_3OD, 300 MHz) (ppm):$\delta = 8.08$ (s, $2H_e$, CH=N), 7.37 (s, $2H_2$, Im ring), 7.09–7.06 (d, $2H_5$, Im ring), 7.00–6.99 (t, $2H_b$, Ar–H), 6.92–6.91 (d, $4H_{a,d}$, Ar–H), 6.60–6.59 (t, $2H_4$, Im), 3.74 (s, 6H, CH_3), 3.59 (s, 6H, OCH_3), 3.31 (d, 2H, chiral H), 2.96–2.92 (d, 2H, CH_2), 2.07–1.51 (m, 6H, CH_2).

Table 1
The crystal data structure parameters for **1c**, **2c** and **3c**

	1c	**2c**	**3c**
Empirical formula	$C_{28.50}H_{34}ClCoN_6O_{6.50}$	$C_{30}H_{36}ClCoN_6O_8$	$C_{44}H_{64}ClCoN_6O_6$
Formula weight	659.00	703.3	867.39
Temperature (K)	293(2)	293(2)	293(2)
Wavelength (Å)	0.71073 (Mo Kα)	0.71073 (Mo Kα)	0.71073 (Mo Kα)
Crystal system	orthorhombic	orthorhombic	orthorhombic
Space group	$P2(1)2(1)2(1)$	$P2(1)2(1)2(1)$	$P2(1)2(1)2(1)$
Unit cell dimensions			
a (Å)	9.306(3)	8.915(3)	9.947(5)
b (Å)	16.174(5)	16.302(5)	15.407(7)
c (Å)	20.566(6)	24.809(8)	31.812(14)
α (°)	90	90	90
β (°)	90	90	90
γ (°)	90	90	90
Volume (Å^3)	3095.4(15)	3606(2)	4875(4)
Z	4	4	4
Calculated density (Mg m^{-3})	1.414	1.295	1.182
Absorption coefficient (mm^{-1})	0.693	0.603	0.455
$F(0\,0\,0)$	1372	1464	1848
Crystal size (mm)	$0.30 \times 0.25 \times 0.20$	$0.30 \times 0.20 \times 0.08$	$0.30 \times 0.2 \times 0.15$
θ Range for data collection (°)	$2.35 \leq \theta \leq 25.02$	$2.5 \leq \theta \leq 25.02$	$1.84 \leq \theta \leq 25.02$
Limiting indices	$-11 \leq h \leq 9$, $-15 \leq k \leq 19$, $-24 \leq l \leq 21$	$-10 \leq h \leq 10$, $-15 \leq k \leq 19$, $-24 \leq l \leq 29$	$-11 \leq h \leq 11$, $-18 \leq k \leq 14$, $-36 \leq l \leq 37$
Reflections collected unique	12757/5408 [$R_{int} = 0.0860$]	14695/6272 [$R_{int} = 0.01622$]	19842/8489 [$R_{int} = 0.0657$]
Completeness to $\theta = 25.02$ (%)	98.8	98.5	98.7
Max/min transmission	0.8738, 0.8190	0.9534, 0.8399	0.9349, 0.8756
Refinement method	full-matrix least-squares on F^2	full-matrix least-squares on F^2	full-matrix least-squares on F^2
Data/restraints/parameters	5408/0/387	6272/0/416	8489/0/523
Final R indices	$R_1 = 0.0578$, $wR_2 = 0.1122$	$R_1 = 0.0694$, $wR_2 = 0.1346$	$R_1 = 0.0616$, $wR_2 = 0.1454$
R indices (all data)	$R_1 = 0.1194$, $wR_2 = 0.1317$	$R_1 = 0.2063$, $wR_2 = 0.1745$	$R_1 = 0.1060$, $wR_2 = 0.1689$
Goodness-of-fit on F^2	0.974	0.958	1.051
Largest difference peak and hole (e Å^{-3})	0.613 and −0.339	0.430 and −0.341	0.823 and −0.415

*2.2.2.7. [Co(t-Bu-Salen)(Im)$_2$]ClO$_4$ complex (**3a**).* To a suspension of the ligand *t*-Bu-Salen and imidazole in methanol (10 ml) was added a solution of NaOH (30 mg, 0.75 mmol) in methanol (2.0 ml). The reaction mixture was stirred for 0.5 h and then $Co(CH_3COO)_2 \cdot 4H_2O$ (0.125 g, 0.5 mmol) was added. The reaction mixture turned purple and stirring was continued for 2 h to give a dark red solution. $NaClO_4 \cdot H_2O$ (0.17 g) in methanol (7 ml) was then added and the mixture was stirred for 20 h. The resulting dark red precipitate was collected by filtration and then was recrystallized from dichloromethane–methanol. Yield: 42.6%. *Anal*. Found: C, 55.58; H, 6.91; N, 9.45. Calc. for $C_{42}H_{60}O_2N_6Co_1 \cdot ClO_4 \cdot CH_2Cl_2$: C, 55.87; H, 6.71; N, 9.10%. FT-IR (KBr, cm^{-1}): 3157 (w, Im ring), 3039 (w, Ar–H), 2952 (s), 2906 (m), 2866 (m, H–C–H), 1626 (vs, C=N), 1545, 1527 (w, Ar, C=C), 1458 (m), 1436 (s, Ar–H), 1386, 1361 (w, C–N), 1325 (s, Ar C–C), 1255 (s, C–O), 1106 (s), 624 (m, ClO_4^-), 541 (m, M–N), 495 (m), 473 (m, M–O). UV–Vis:λ_{max} (nm) (log(ε, M^{-1} cm^{-1}) (CH_2Cl_2): 425.4 (3.75), 270 (4.45), 234 (4.36). CD

Table 2
Selected angles (°) and bond lengths (Å) of complexes for **1c**, **2c** and **3c**

	1c	**2c**	**3c**
Bond angles			
O(1)–Co(1)–N(1)	94.8(2)	95.1(3)	95.50(16)
N(1)–Co(1)–N(2)	85.5(2)	85.4(3)	85.21(17)
O(2)–Co(1)–N(2)	93.72(19)	94.5(3)	94.59(16)
N(2)–Co(1)–O(1)	176.95(19)	178.1(3)	177.10(18)
N(1)–Co(1)–O(2)	178.7(2)	177.4(3)	176.05(18)
O(1)–Co(1)–O(2)	86.06(19)	85.1(3)	85.89(14)
N(2)–Co(1)–N(3)	89.8(3)	92.7(3)	89.01(18)
N(2)–Co(1)–N(5)	94.0(2)	91.0(3)	92.71(18)
N(1)–Co(1)–N(5)	89.8(2)	93.0(3)	88.16(18)
N(1)–Co(1)–N(3)	92.22(19)	89.2(3)	93.91(18)
N(3)–Co(1)–N(5)	175.9(3)	175.9(3)	177.42(19)
Bond lenghts			
Co(1)–O(2)	1.885(4)	1.878(6)	1.883(3)
Co(1)–O(1)	1.896(4)	1.879(6)	1.881(3)
Co(1)–N(1)	1.890(5)	1.890(7)	1.882(4)
Co(1)–N(2)	1.893(5)	1.916(7)	1.869(4)
Co(1)–N(3)	1.938(4)	1.935(8)	1.938(5)
Co(1)–N(5)	1.961(5)	1.933(8)	1.930(4)

(CH_2Cl_2) λ_{max} (nm), ($\Delta\varepsilon$, $M^{-1}\,cm^{-1}$): 550 (+25.5), 431 (−113.9), 377 (−1.99), 340 (−18.9), 306 (−17.3), 280 (−6.24), 262 (−13.14). ^1H NMR (CD_3OD, 300 MHz) (ppm):$\delta = 8.11$ (s, 2H, CH=N), 7.42 (s, 2He, Im ring), 7.41–7.26 (s, $2H_b$, Ar–H), 7.30–7.29 (d, $2H_d$, Ar–H), 6.91–6.90 (d, $2H_5$, Im ring), 6.51 (s, $2H_4$, Im ring), 3.20 (s, 2H, chiral H), 2.96–2.95 (d, 2H, CH_2), 2.06–1.47 (m, 6H, CH_2), 1.37 (s, 9H, *t*-Bu), 1.32 (s, 9H, *t*-Bu).

*2.2.2.8. [Co(t-Bu-Salen)(2-MeIm)$_2$]ClO$_4$ complex (**3b**).* The complex was prepared by the same method as for **3a** except that ethanol was used as the solvent and 2-methylimidazole was used instead of imidazole. Recrystallization from dichloromethane–ethanol gave a dark red solid. Yield: 68%. *Anal*. Found: C, 60.58; H, 7.64; N, 9.16. Calc. for $C_{44}H_{64}O_2N_6Co_1{\cdot}ClO_4$: C, 60.94; H, 7.39; N, 9.69%. FT-IR (KBr, cm^{-1}): 3132 (w, Im

$[Co(Salen)(MeIm)_2]ClO_4.CH_3OH$ (**1c**)

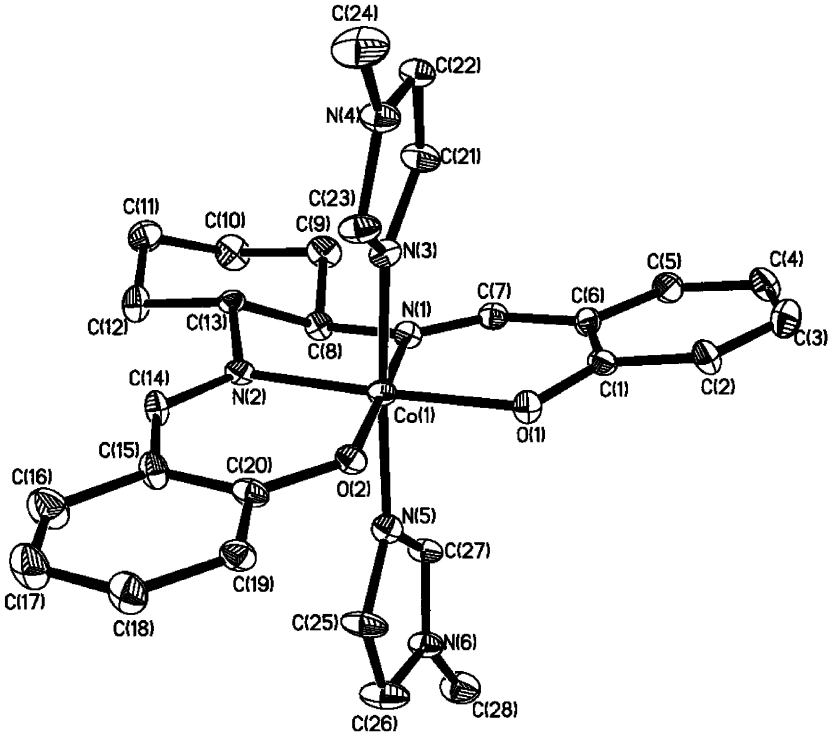

$[Co(MeOSalen)(MeIm)_2]ClO_4$ (**2c**)

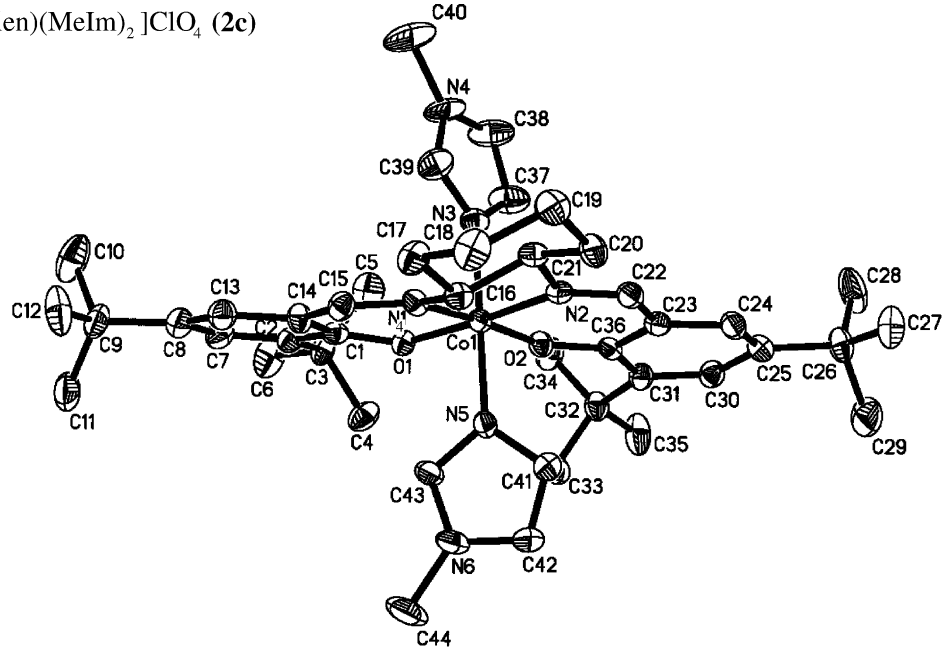

Fig. 2. ORTEP diagrams for **1c**, **2c** and **3c**.

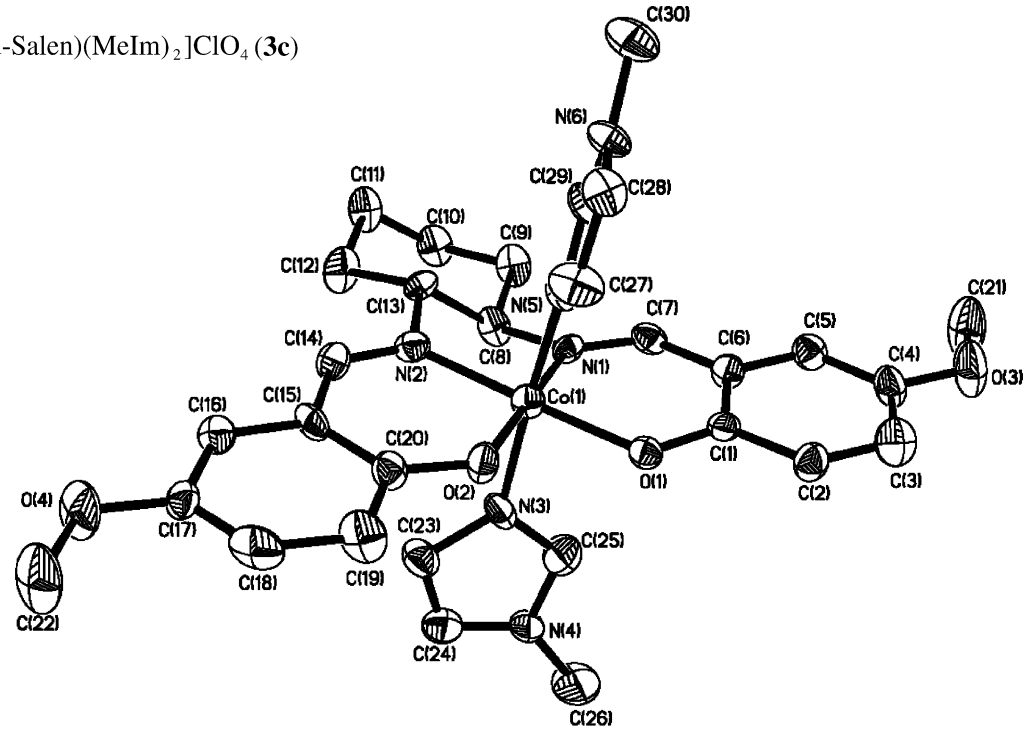

Fig. 2 (*Continued*)

ring), 3052 (w, Ar–H), 2961 (s), 2935 (m), 2864 (m, H–C–H), 1630 (vs, C=N), 1593 (w, Ar C=C), 1468 (w), 1438 (s, Ar–H), 1390 (w, C–N), 1361(s), 1303 (m, Ar C–C), 1270 (m), 1240 (w, C–O), 1085 (s, ClO_4^-), 664 (w, M–N), 424 (m, M–O). UV–Vis λ_{max} (nm) (log(ε, M^{-1} cm^{-1})) (CH_2Cl_2): 414 (3.80), 272 (4.43), 235 (4.33). CD λ_{max} (nm) ($\Delta\varepsilon$, M^{-1} cm^{-1}) (CH_2Cl_2): 635 (+6.42), 431 (−8.0), 390 (−3.36), 341 (−6.61), 300 (−4.28), 275 (−7.10), 230 (2.54).

*2.2.2.9. [Co(t-Bu-Salen)(MeIm)$_2$]ClO$_4$ complex (**3c**).* This dark red complex was prepared by the same method as for **3a** except that 1-methylimidazole was used instead of imidazole. The product was recrystallized from dichloromethane–methanol. Yield: 64%. *Anal.* Found: C, 60.23; H, 6.78; N, 9.74. Calc. for $C_{44}H_{64}O_2N_6Co_1 \cdot ClO_4$: C, 60.94; H, 7.39; N, 9.69%. FT-IR (KBr, cm^{-1}): 3159 (m, Im ring), 3039 (w, Ar–H), 2952 (s), 2907 (m), 2867 (w, H–C–H), 1628 (vs, C=N), 1528 (s, Ar, C=C), 1458 (w), 1436 (s, Ar–H), 1340 (m, C–N), 1361 (m), 1324 (s, Ar C–C), 1255 (s), 1238 (m, C–O), 1097, 622 (s, ClO_4^-), 569 (m, M–N), 496 (m), 474 (m, M–O). UV–Vis λ_{max} (nm) (log(ε, M^{-1} cm^{-1})) (CH_2Cl_2): 422 (3.82), 271 (4.46), 234 (4.33). CD λ_{max} (nm), ($\Delta\varepsilon$, M^{-1} cm^{-1}), (CH_2Cl_2): 556 (+46.98), 433 (−113.9), 380 (−0.76), 341 (−39.0), 320 (−28.99), 308 (−34.3). ^{1}H NMR (CD_3OD, 300 MHz) (ppm):$\delta = 8.13$ (s, $2H_e$, CH=N), 7.46–7.45 (d, $2H_2$, Im ring), 7.30–7.29 (d, $2H_b$, Ar–H), 7.25 (s, $2H_d$, Ar–H), 6.92–6.91 (t, $2H_5$, Ar–H), 6.54–6.52 (t, $2H_4$, Im ring), 3.58 (s, 6H, CH_3), 3.30–3.27 (m, 2H, chiral H), 3.02–2.98 (d, 2H, CH_2), 2.08–1.51 (m, 6H, CH_2), 1.44 (s, 9H, *t*-Bu), 1.36 (s, 9H, *t*-Bu).

2.3. Crystallography

The crystal data of **1c**, **2c** and **3c** are listed in Table 1. The determination of unit cell parameters and data collections on a Bruker Smart 1000 CCD diffractometer were performed with Mo Kα radiation ($\lambda = 0.71073$ Å) at 298(2) K.

Semi-empirical absorption was applied using SADABS method and the structures were solved by direct methods using the SHELXL-97 program [17]. The non-hydrogen atoms were refined anisotropically by full-matrix least-squares on F^2. The generated hydrogen atoms were refined with fixed thermal factors. The refinement parameters for **1c**, **2c** and **3c** are listed in Table 2.

3. Results and discussion

3.1. Crystal structure

The molecular structure of complexes **1c**, **2c** and **3c** are shown in Fig. 2. Cobalt complexes **1c**, **2c** and **3c** are composed of the cation $[Co(Salen)(MeIm)_2]^+$, $[Co(MeO\text{-}Salen)(MeIm)_2]^+$ and $[Co(t\text{-}Bu\text{-}Salen)(MeIm)_2^+$, respectively, and the anion ClO_4^-. The co-

existing MeOH molecule found in the structure of **1c** does not participate in coordination.

The cobalt(III) center is coordinated by two oxygen atoms and two nitrogen atoms from the Salen complex and two additional nitrogen atoms from the axial ligand 1-methylimidazole, forming an octahedral coordination geometry. The two axial ligands are approximately normal to the Salen plane. (Table 2) The axial bond angle N(3)–Co–N(5) in the octahedron are 177.4(2)° for **3c** and 175.9(2)° for both **1c** and **2c**. The probable reason for the difference is the influence of the substituents on the Salen ring. Complex **3c** has bulky *tert*-butyl groups on the 3,5-positions of the Salen ring, while complex **1c** has none and **2c** has a methoxyl group on the 5-position, which has no major influence on the axial ligands. The steric effect of the *tert*-butyl group causes the axial ligand to get closer to metal center resulting in a slightly larger angle.

The Co–O(1) and Co–O(2) bond lengths for the three complexes are similar (Table 2), ranging from 1.878(6)

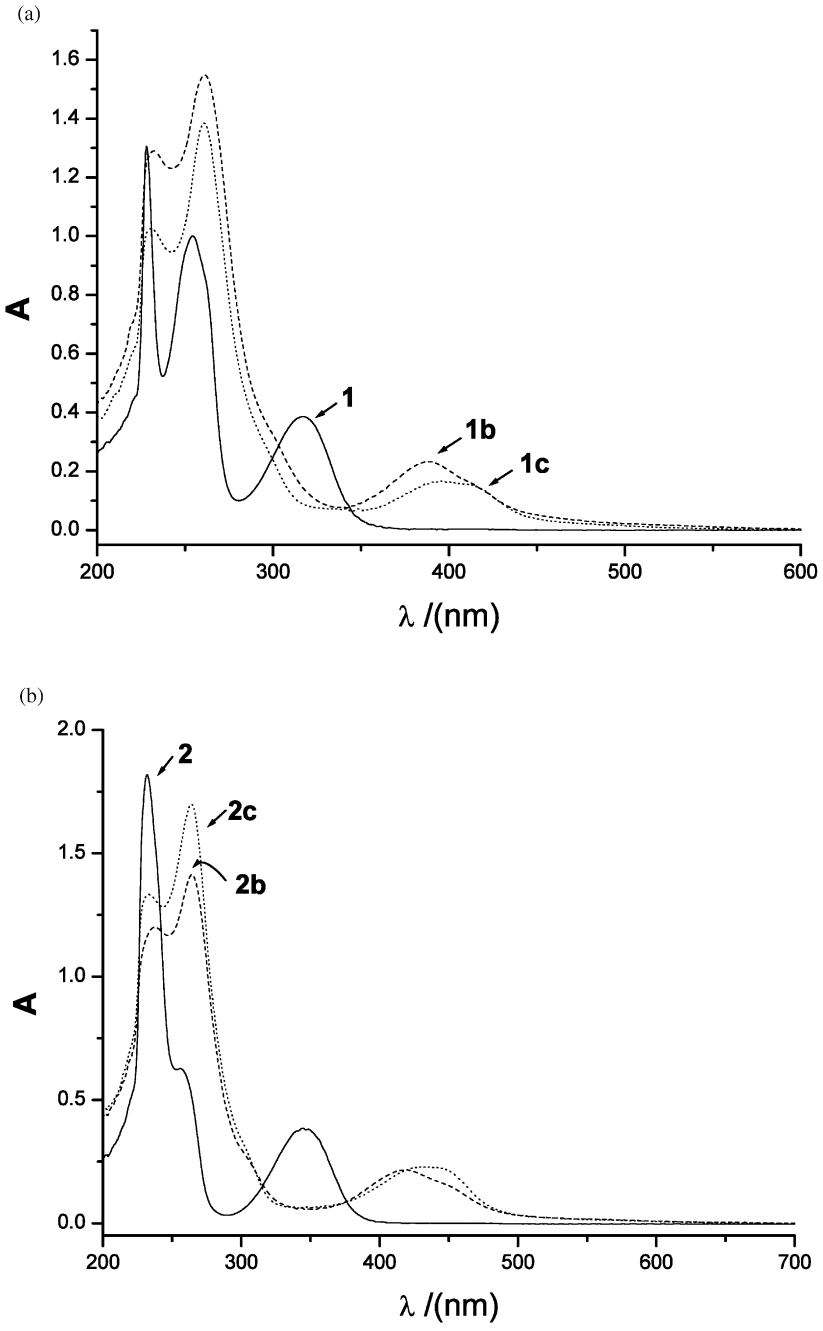

Fig. 3. The UV–Vis spectra of ligands (**1**, **2**, **3**) and complexes. (a) Ligand Salen **1** and its complexes $[Co(salen)(2\text{-}MeIm)_2]ClO_4$ (**1b**),[Co(Salen)(MeIm)2](ClO_4 (**1c**). (b) Ligand MeOsalen **2** and its complexes [Co(salen)(2-MeIm)2]ClO_4 (**2b**), [Co(MeOSalen)(2-MeIm)2]ClO_4 (**2c**).

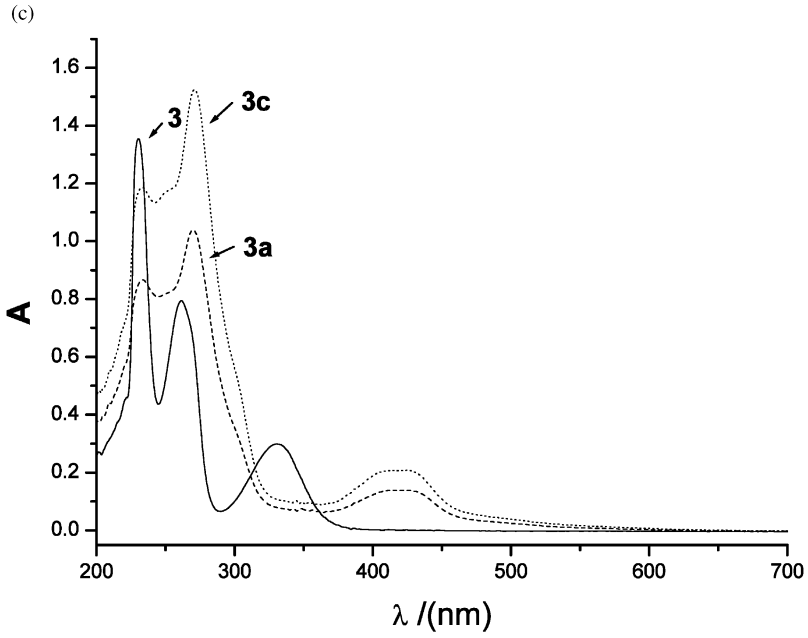

Fig. 3 (*Continued*)

to 1.896(4) Å, which is in good agreement with those in the literature. The Co–N(1) and Co–N(2) bond distances are also close to those in the literature [2,3,18]. The Co–N(3) and Co–N(5) bond distances are close to each other for **3c** and **2c** (**3c**, 1.930(4), 1.938(5); **2c**, 1.933(8), 1.935(8)) but show a larger difference for **1c** (1.938(4), 1.962(5)), which can be explained by the effect of the solvent molecule MeOH in the structure. From Table 2, we also see that the Co–N(1) and Co–N(2) bond distances are shorter than the Co–N(3) and Co–N(5) bond distances by 0.019–0.079 Å, which is caused by the different chiral skeleton structure of the ligands.

3.2. FT-IR spectra

The IR spectra of the complexes show two weak bands at 2960 and 2860 cm^{-1} which can be attributed to CH_2 stretching vibration. An intensive band at 1640–1610 cm^{-1} is characteristic of the conjugated C=N stretching vibration. The stronger band in the 1600–1500 cm^{-1} is due to the skeleton stretching vibration of C=C of the benzene ring. On the other hand, near 1100 and 620 cm^{-1}, those very strong and mild intensity bands are ascribed to the stretching vibration of ClO_4^- [19].

3.3. H NMR spectra

The ^1H NMR spectral data are presented in Section 2. For the free ligands, the lowfield signal which appears at $\delta = 13.0$, due to extensive hydroxyl formation, disappears in the cobalt complexes. The aromatic protons of all axial coordination cobalt complexes are generally shifted to lower fields compared with the relevant Salen ligands. The proton signals of axial imidazoles are shifted to higher fields relative to those of the free imidazoles. Using $[Co(MeOSalen)(MeIm)_2]ClO_4$ (**2c**) complex as an example, the proton signals of axial ligand 1-methylimidazole appear at 7.37, 6.92–6.91, 6.60–6.59, 3.74 ppm while those of the free ligand 1-methylimidazol appear at 7.62, 7.10, 6.98, 3.76 ppm.

3.4. UV–Vis and CD spectra

For the free Salen ligand, as shown in Fig. 3, the band in the region of 300–450 nm in UV–Vis spectra is attributed to a π–π* transition of the azomethine chromophore, and the bands in the higher energy region at 200–300 nm to the π–π* transition of the benzene ring of salicylaldehyde [19,20]. For axial coordination Salen cobalt complexes, however, all bands are assigned to a π–π* transition with a bathochromic shift (also see Fig. 3). The differences between the cobalt complexes and the free ligands in UV–Vis spectra are attributed to the π–π* transition of the ligand. Co(III) ions are rigidly linked in the N–M–N bond, leading to an increase of conjugation in a molecule [19,21]. The d–d bands are not observed due to the low concentration ($\sim 10^{-4}$ mol dm^{-3}) of the complexes solution. These bands should be low in intensity in the region of 500–600 nm.

As shown in the CD spectra (Fig. 4), bands are found at 353 and 382 nm(−) with negative Cotton effect for free ligands Salen **1** and *t*-Bu-Salen **3e**, respectively. For ligand 2, MeOSalen, the absorption band 383 nm(−) is attributed to the split π–π* transition of azomethine and low energy absorption spectra [20]. In addition, the

peaks at 300 nm(−), 283 nm(+) are also shown in CD spectrum.

These metal cobalt(III) complexes have an analogous structure so that they have similar CD spectra in dichloromethane solution. The CD spectra in the 500–600 nm region exhibit the positive Cotton effect, which can be ascribed to a d–d transition of metal cobalt [20,21]. The CD spectra split into a stronger negative Cotton effect at 400–500 nm, which is considered to be the result of the electron transitions from the ligand π orbit and oxygen nonbonding orbit to the strong antibonding 3d orbit. The other two electronic absorption bands at high energy (below 400 nm) which are considered to be the π–π* transition of the azomethine

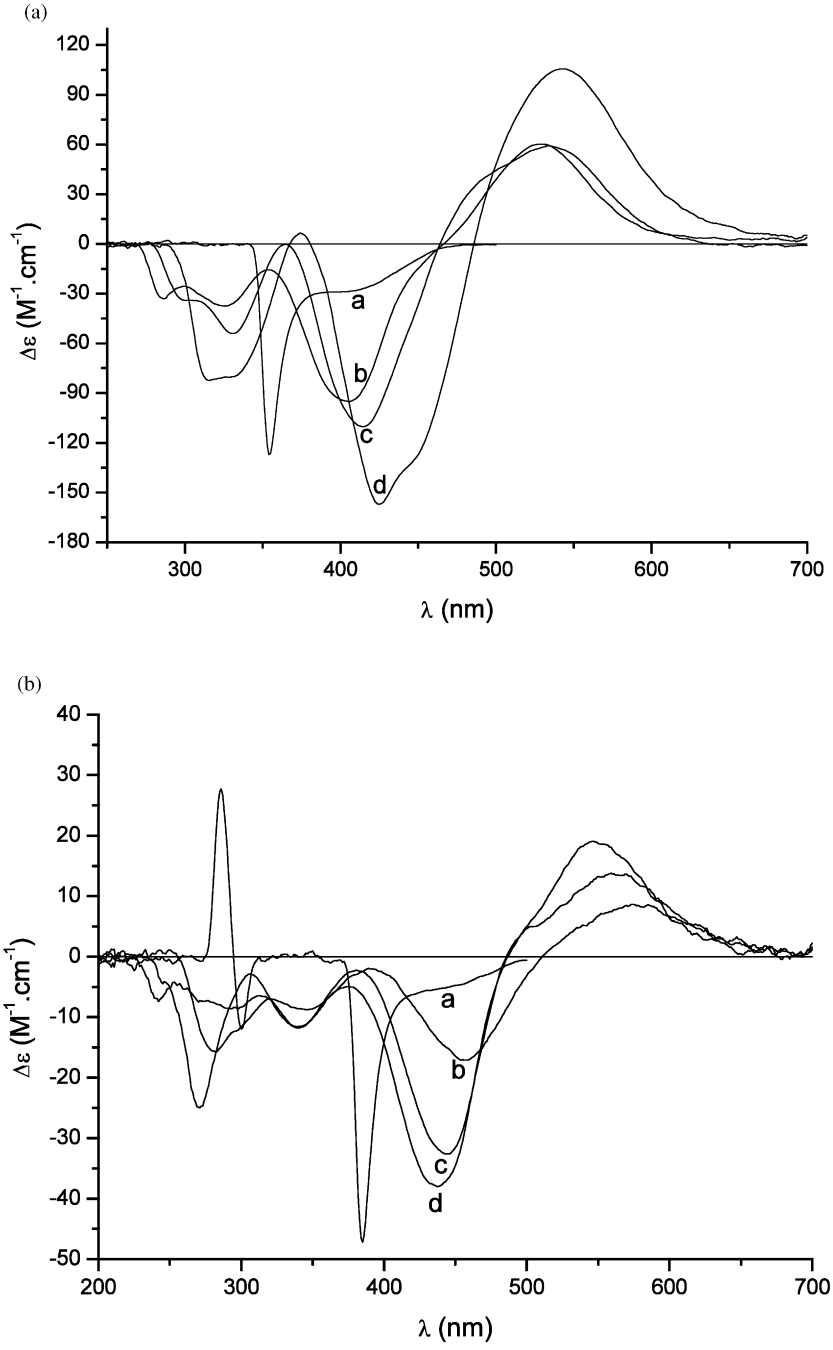

Fig. 4. The CD spectra of ligands (**1**, **2**, **3**) and complexes. (a) Ligand Salen **1** and itscomplexes $[Co(Salen)(Im)_2]C1O_4$ (b),$[Co(Salen)(MeIm)_2]C1O_4$ (c), $[Co(Salen)(MeIm)_2]C1O_4$ (d). (b) Ligand MeOSalen **2** and its complexes $[Co(Salen)(2\text{-}MeIm)_2]C1O_4$ (b), $[Co(MeOSalen)(MeIIm)_2]C1O_4$ (c), $[Co(MeOSalen)(Im)_2]C1O_4$ (d).

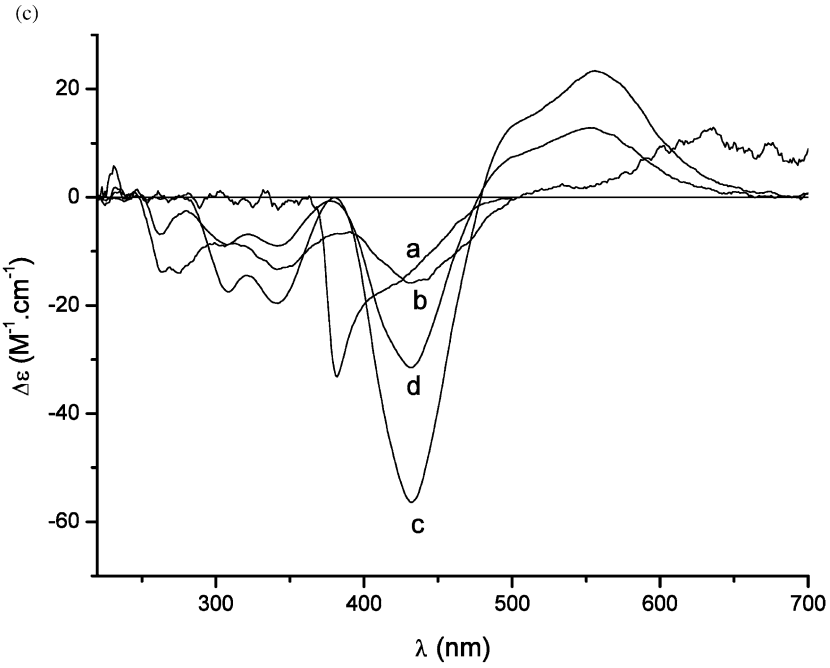

Fig. 4 (*Continued*)

groups and the benzene ring show a weaker negative Cotton effect and a medium intensity negative Cotton effect in CD spectra. The resulting coupling-split of the complexes is caused by the effect of the central chelate ring N–O–O–N whose configuration has been determined [21,22]. For hexacoordinate Co complexes, the O_2N_2 chelate ring is linked with the cobalt ion in a nearly square plane. The sixth coordinated atom in the axial position does not influence the configuration of chelated ring [20,22]. It is predicted that when the chirality configuration is Λ [21] (IUPAC nomenclature [23]), the negative component of the azomethine π–π* couplet will lie at higher energy, whereas the lower energy case corresponds to the configuration Δ. A molecular model shows that the ligand of (*R*, *R*)-Salen coordinated to cobalt stereospecificially conforms to the Δ configuration [21,24]. Therefore, the CD spectra will show a negative Cotton effect at long wavelength.

4. Supplementary material

Crystallographic data for the structural analysis have been deposited with the Cambridge Crystallographic Data Centre, CCDC Nos. 199364 for compound **1c**, 199363 for compound **2c**, 199365 for compound **3c**. Copies of this information may be obtained free of charge from The Director, CCDC, 12 Union Road, Cambridge, CB2 1EZ, UK (fax: +44-1223-336033; e-mail: deposit@ccdc.cam.ac.uk or www: http://www.ccdc.cam.ac.uk).

Acknowledgements

This work is supported by the National Natural Science Foundation (Grant No. 20171024, 20271030), the Tianjin Natural Science Foundation (No. 023604011), and the Research Fund for Returning Scholars from Abroad.

References

[1] E.C. Niederhoffer, J.H. Timmons, A.E. Martell, Chem. Rev. 84 (1984) 137.
[2] M. Hirotsu, M. Kojima, K. Nakajima, Bull. Chem. Soc. Jpn 69 (1996) 2549.
[3] M. Amirnasr, K.J. Schenk, A. Gorji, R. Vafazadef, Polyhedron 20 (2001) 695.
[4] M.M. Aly, J. Coord. Chem. 43 (1998) 89.
[5] R. Cmi, S.J. Moore, L.G. Marzilli, Inorg. Chem. 37 (1998) 6890.
[6] S.M. Polson, R. Cini, C. Pifferi, L.G. Marzilli, Inorg.Chem. 36 (1997) 314.
[7] S. Yamada, Coord. Chem. Rev. 191–192 (1999) 537.
[8] N.J. Henson, P.J. Hay, A. Redondo, Inorg. Chem. 38 (1999) 1618.
[9] C. Bianchini, R.W. Zoeliner, Adv. Inorg. Chem. 44 (1997) 263.
[10] A. Botteher, T. Takeuchi, K.I. Hardcastle, T.J. Meade, H.B. Gray, Inorg. Chem. 36 (1997) 2498.
[11] E.N. Jacobsen, W. Zhang, M.L. Guler, J. Am. Chem. Soc. 113 (1991) 6703.
[12] B. Speiser, H. Stahl, Angew. Chem. Int. Ed. Engl. 34 (1995) 1086.
[13] N. Nishinaga, H. Tomita, J. Mol. Catal. 7 (1980) 178.
[14] Y.-J. Hu, X.-D. Huang, Z.-J. Yao, Y.-L. Wu, J. Org. Chem. 63 (1998) 2456.
[15] J.F. Larrow, E.N. Jacobsen, J. Org. Chem. 59 (1994) 1939.
[16] F. Galsbol, P. Steenbol, S. Sondergaard, Acta Chem. Scand. 26 (1972) 3605.

[17] E. Kitaula, Y. Nishida, H. Okawa, S. Kida, J. Chem. Soc., Dalton. Trans. 12 (1987) 3055.
[18] G.M. Sheldrick, SHEXLS-97, Program for X-ray Crystal Structure Solution, Göttingen University, Germany, 1997.
[19] R.C. Felicio, E.T.G. Canalheiro, E.R. Dockal, Polyhedron 20 (2001) 261.
[20] S. Zolezzi, A. Decinti, E. Spodine, Polyhedron 18 (1999) 897.
[21] A. Wojtczak, E. Sylyk, M. Jaskolski, E. Larsen, Acta Chem. Scand. 51 (1997) 274.
[22] R.S. Downing, F.L. Urbach, J. Am. Chem. Soc. 91 (1969) 5977.
[23] J. Fujita, Y. Shimura, in: K. Nakamoto, P.J. Mccarthy (Eds.), Spectroscopy and Structure of Metal Chelate Compounds (chapter 3), Wiley, New York, 1968.
[24] M.J. O'Connor, R.E. Ernst, R.H. Holm, J. Am. Chem. Soc. 90 (1968) 4561.